Research article

JHEP|Reports

Hepatic stellate cell single cell atlas reveals a highly similar activation process across liver disease aetiologies

Vincent Merens[1], Elisabeth Knetemann[1], Elif Gürbüz[1], Vincent De Smet[1,2], Nouredin Messaoudi[2], Hendrik Reynaert[1,2], Stefaan Verhulst[1,*,‡], Leo A. van Grunsven[1,*,‡]

JHEP Reports **2025**. vol. 7 | 1–12

Background & Aims: The progression of chronic liver disease (CLD) is characterized by excessive extracellular matrix deposition, disrupting hepatic architecture and function. Upon liver injury, hepatic stellate cells (HSCs) differentiate towards myofibroblasts and become inflammatory, proliferative and fibrogenic. To date, it is still unclear whether HSC activation is driven by similar mechanisms in different aetiologies.

Methods: HSCs from multiple publicly available single-cell RNA-sequencing datasets were annotated and merged into a single-cell HSC activation atlas. Spheroid co-cultures of primary mouse hepatocytes/HSCs (n = 5) and ELISAs on patient plasma samples (n = 80) were performed to validate the mechanistic insight obtained from the HSC atlas.

Results: We established an HSC activation atlas in which HSCs are clearly divided into three distinct transcriptomic profiles: quiescent HSCs, initiatory HSCs and myofibroblasts. These transcriptomic profiles are present in each of the investigated mouse liver injury models as well as in human CLDs, indicating that HSC activation is a conserved process. This activation process is driven by a core set of transcription factors independent of liver injury or species. Furthermore, we reveal novel ligands associated with activation of HSCs in multiple liver injury models and validate the profibrotic effect of parathyroid hormone. Finally, we identify *COLEC10* as a conserved marker for quiescent HSCs and a biomarker of liver fibrosis in patients with different CLDs (p <0.0001).

Conclusions: We reveal unexpected similarities in the regulatory mechanisms of HSCs across diverse liver injury settings and species. The HSC activation atlas has the potential to provide novel insights into liver fibrosis and steer novel treatment options.

Introduction

Chronic liver disease (CLD) is a major health burden, with cirrhosis and liver cancer causing 2 million deaths globally each year.[1] While the prevalence of CLD is increasing due to an aging population and an increase in metabolic dysfunction-associated steatotic liver disease (MASLD), there are still no approved drugs available in the clinic that target liver fibrosis.

CLD can be caused by a broad range of injuries, and a range of murine models has been developed to reflect this diversity. Hepatotoxic injury models like carbon tetrachloride (CCl_4) injection[2] and western diet[3] are used to model hepatocellular damage such as drug-induced liver injury and MASLD, while cholestatic injury models like bile duct ligation (BDL)[4] are used to model chronic cholestatic damage. In both hepatotoxic and cholestatic liver injury models, hepatic stellate cells (HSC) are the dominant extracellular matrix-producing cell type at later stages of injury.[5]

In recent years, single-cell RNA sequencing (scRNA-Seq) studies have demonstrated a large heterogeneity within cell types which sometimes reflects the transition between cell states at single-cell resolution. Currently, the heterogeneity and zonation of several liver-specific cell types have been described in different mouse and human liver injuries, with a great emphasis on endothelial and hepatocyte zonation as well as macrophage differentiation. Individual scRNA-Seq studies have identified HSC heterogeneity and zonation and identified the peri-central HSCs as the major source of myofibroblasts in CCl_4-induced liver fibrosis.[2–4,6–12] However, it is still unclear whether the mechanisms that drive HSC activation depend on the kind of liver injury, *i.e.* cell death by CCl_4 or BDL, lipid overload of hepatocytes by a western diet, or recruitment to cancer cells to act as cancer-associated fibroblasts. Equally important is the question of whether these mechanisms are different depending on the organism and stage of fibrogenesis (acute *vs.* chronic).

Here, we constructed a single-cell atlas of HSCs by integrating 10 different scRNA-Seq datasets representing seven different mouse liver injury models. The HSC atlas identifies a strongly conserved HSC activation process among liver injuries, stages and species, which is driven by a limited set of upstream signalling events and transcription factors (TFs). This

* Corresponding author. Address: Vrije Universiteit Brussel, Liver Cell Biology research group, Laarbeeklaan 103, 1090 Brussel, Belgium.
E-mail addresses: Stefaan.Verhulst@vub.be (S. Verhulst), Leo.van.Grunsven@vub.be (L.A. van Grunsven).
‡ Equal contribution senior authors
https://doi.org/10.1016/j.jhepr.2024.101223

has great implications for the future development and testing of anti-fibrotic drugs aiming to target HSCs. Additionally, through the use of the HSC activation atlas we pinpoint and validate *COLEC10* as a novel biomarker to stage liver fibrosis in patients with CLD and identify parathyroid hormone as a novel ligand inducing HSC activation. Finally, we provide two easy-to-use web applications; one to browse the single-cell HSC atlas for your gene of interest and another tool that can annotate HSCs within single-cell or single-nuclei RNA-Seq datasets. The latter identifies mesenchymal cells, extracts HSC populations and annotates them based on their quiescent-, initiatory- or myofibroblast phenotype.

Materials and methods

Atlas construction

Generation of the mouse HSC activation atlases was based on scRNA-Seq datasets from seven studies describing 10 different murine liver injury datasets (Table S1).[2–4,6–9] For the human HSC activation atlas, we included three human scRNA-Seq datasets, together representing healthy and injured livers (Table S2).[10–12] Details regarding the generation and analysis of the HSC atlases are described in the supplementary information.

Patient cohort

Patients for this study were enlisted from the Department of Gastroenterology at the University Hospital of Brussels (UZ Brussel), Belgium. Approval for the study protocol was obtained from the local ethical committee of both UZ Brussel and Vrije Universiteit Brussel (reference number 2015/297; B.U.N. 143201525482) and complied with the Declaration of Helsinki. For inclusion criteria see supplementary information.

Blood collection and COLEC10 ELISA

Venous blood samples were obtained through venepuncture, collected in evacuated EDTA-KE S-Monovette tubes (Sarstedt AG & Co) on the day of either liver biopsy or elastography. Blood specimens underwent standard comprehensive haematological and biochemical analyses. To generate plasma, a two-step centrifugation protocol was employed, involving 1,500 g for 10 min at 4 °C, followed by 2,000 g for 3 min at 4 °C and stored at −80 °C. COLEC10 plasma levels were measured with an ELISA kit (AssayGenie, HUFI02333) at an 1/50 dilution using an iMark microplate absorbance reader (Bio-rad) at 450 nm. Receiver-operating characteristic curves were constructed with the plotROC package in R.[13]

Mice

Male BALB/c mice at an age of 13 to 24 weeks were used for all experiments (Charles River Laboratories). Mice were fed *ad libitum*. All experiments were approved by the Ethics Committee of Animal Testing of Vrije Universiteit Brussel (20-212-5) and were carried out in accordance with the ARRIVE guidelines.

Primary mouse HSC-hepatocyte spheroids

Primary mouse hepatocytes and HSCs were isolated as described by van Os *et al.*[14] and cultured in Nunclon Sphera-Treated, U-Shaped-Bottom Microplate (Thermo Fisher Scientific) at a ratio of 1:2 respectively with a density of 2,000 total cells per well with orbital shaking (Infors Celltron). See supplementary information for details. At day 3 and 5, 100 µl of media was replaced by 100 µl of media containing solvent, 5 ng/ml TGF-β or 80 nM parathyroid hormone (Bio-Legend, 753202).

RNA extraction, reverse transcription and quantitative PCR

Total RNA was extracted from the primary mouse HSC-hepatocyte spheroids with a ReliaPrep RNA Cell Miniprep System (Promega) and reverse transcribed using MLV reverse transcriptase (Promega). GoTaq qPCR Master Mix with BRYTE green (Promega) was used for quantitative real-time PCR using specific primers (Integrated DNA Technologies, Table S3) and analysed by a Quantstudio3 Fast PCR system (Thermo Fisher Scientific). Samples were normalised against *Desmin* and analysed according to the comparative Ct method (Δ ΔCT).[15]

Fixation, staining and immunofluorescence

Spheroids were washed with PBS, fixed with 4% formalin (Merck) at room temperature for 10 min, washed 3 times with PBS before embedding in paraffin or whole spheroid staining. For Sirius red staining, spheroids were cut into 5 µm thick sections, incubated for 1 h with 0.1% (w/v) Sirius red (Sigma-Aldrich) phase green in a saturated picric acid solution. Images were analysed for the percentage Sirius red-positive area with QuPath.[16] For immunostaining, whole spheroids were stained with HNF4A antibody (Abcam, ab41898; 1/200) and Desmin antibody (Epredia, RB-9014-P1; 1/200) followed by donkey anti-mouse Alexa Fluor 647 and goat anti-rabbit Alexa Fluor 488 (Thermo Fisher Scientific, A31571 & A11008, 1/200).[17]

Results

Mesenchymal atlas

To investigate whether HSCs activate differently depending on the kind of liver injury, we selected 10 scRNA-seq datasets from seven different studies including acute and chronic acetaminophen (APAP), thioacetamide or CCl_4 treatments, BDL mice, mice that had received a western diet and mice suffering from an intrahepatic cholangiocarcinoma (Fig. S1A, Table S1).[2–4,6–9] Mesenchymal cells were identified in all studies by expression of *Pdgfrb* (Fig. 1A and Fig. S1B,C) and a total of 108,366 mesenchymal cells were merged into one dataset (Fig. 1A and Fig. S1D). Conventional markers revealed HSCs, vascular smooth muscle cells, portal fibroblasts, mesothelial cells and endothelial cells, and proliferating cells (Fig. 1A,B). Integrating multiple datasets improved the identification of liver cell types, *e.g.* after integration mesothelial cells can be identified in five different studies by expression of *Upk3b* while previously mesothelial cells were only identified in one of these studies (Fig. S2).[9] Interestingly, there is an endothelial cell cluster with high expression of both HSC and LSEC (liver sinusoidal endothelial cell) markers (Fig. 1B). Since *Lrat* and *Pecam1* mark different cell populations, we assume that this population consists mostly of doublets (Fig. 1C).[18] In addition, this cluster expresses a higher number of unique genes compared to other clusters (Fig. 1C). Thus, integration of the *Pdgfrb*$^+$ cells of multiple datasets permitted us to more effectively distinguish between mesenchymal cell types and eliminate potential doublet artifacts.

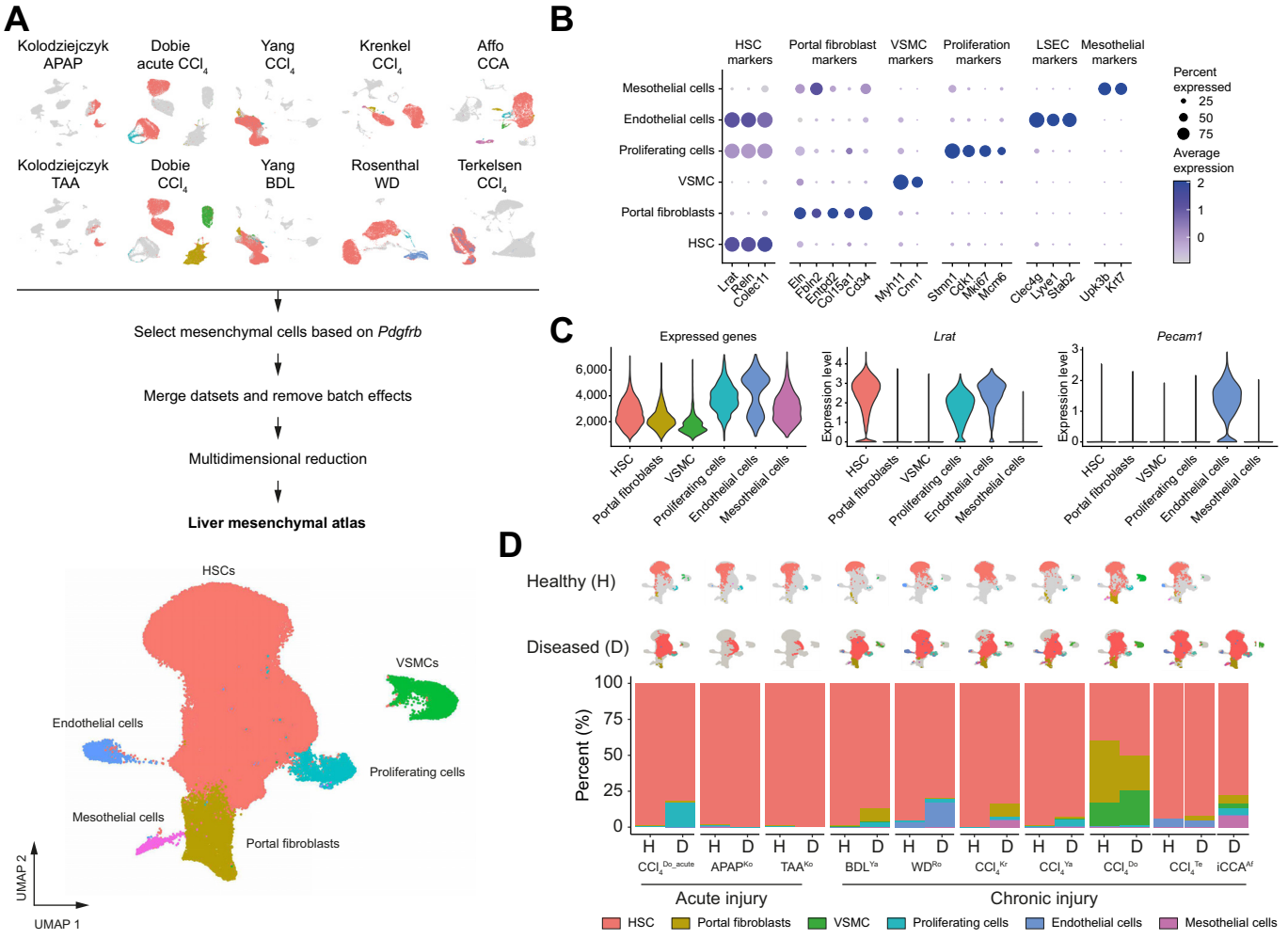

Fig. 1. Mesenchymal liver cell atlas integrating 10 distinct liver injury datasets. (A) Overview of the integration workflow. Top: UMAP plots of 10 different scRNA-Seq datasets. Coloured cells indicate Pdgfrb^{+} cells selected for integration and corresponds to their cell type annotation after further downstream analysis. Bottom: UMAP plot of all integrated Pdgfrb^{+} cells. (B) Expression of cell type specific markers per cluster of the integrated Pdgfrb^{+} cells. (C) Number of expressed genes per cell type and normalized expression of Lrat and Pecam1 per cell type. (D) UMAP and cell type composition of the healthy and injured liver cells per dataset. ScRNA-Seq, single-cell RNA sequencing; UMAP, uniform manifold approximation and projection.

A closer look at the cell type composition of each liver injury separately shows that HSCs are the most abundant mesenchymal cell type in each study and that the presence of other cell types varies significantly between studies (Fig. 1D) depending on isolation method and liver injury model used (Table S1). For instance, cells isolated from CCl_4-injected mice in Dobie *et al.*[2] consist of proportionally more portal fibroblasts and vascular smooth muscle cells than any other study, which can be related to the use of a *Pdgfrb* reporter mice strain to isolate all mesenchymal cells compared to using UV^{+} or gradient separation to isolate only HSCs. In this dataset there are also no LSEC marker-positive HSCs as they exclude ICAM2^{+} cells through FACS sorting. In BDL mice, we find proportionally more portal fibroblasts compared to CCl_4 conditions in the same study (BDL^{Ya} *vs.* $CCl_4{}^{Ya}$), confirming that the method of liver injury influences cell type composition.[4] Cells are clustered by cell type and not by dataset, indicating that the removal of batch effects retained the biological variation and predominantly removed technical variations (Fig. 1D and Fig. S1D).

HSC activation atlas

Next, the HSC cluster was extracted from the mesenchymal atlas and subjected to reclustering. We eliminated "inactivating" HSCs that contain HSCs from the Rosenthal *et al.* study which were isolated from mice after a 2-month recovery period from a high fat diet (Fig. S3, Supplementary File 1). This allowed us to build a single-cell HSC activation atlas (57,233 cells) with three HSC subtypes: quiescent HSCs (qHSCs), initiatory HSCs and myofibroblasts (Fig. 2A). Each HSC subtype expresses a particular set of genes that is conserved in all investigated liver injury models (Fig. 2B and Fig. S4A,B, Supplementary File 2). HSCs from healthy mice are primarily identified as qHSCs, while HSCs isolated after an acute or chronic liver injury are primarily identified as initiatory HSCs and myofibroblasts, respectively (Fig. 2C and Fig. S5). HSCs isolated after one CCl_4 injection (acute CCl_4) have less initiatory HSCs and more myofibroblasts compared to those isolated after single APAP and thioacetamide injections (Fig. S5B), possibly due to a later collection time after the injection (3 days *vs.* 1 day, respectively, Table S1). Zonation was clearly visible in the quiescent cluster

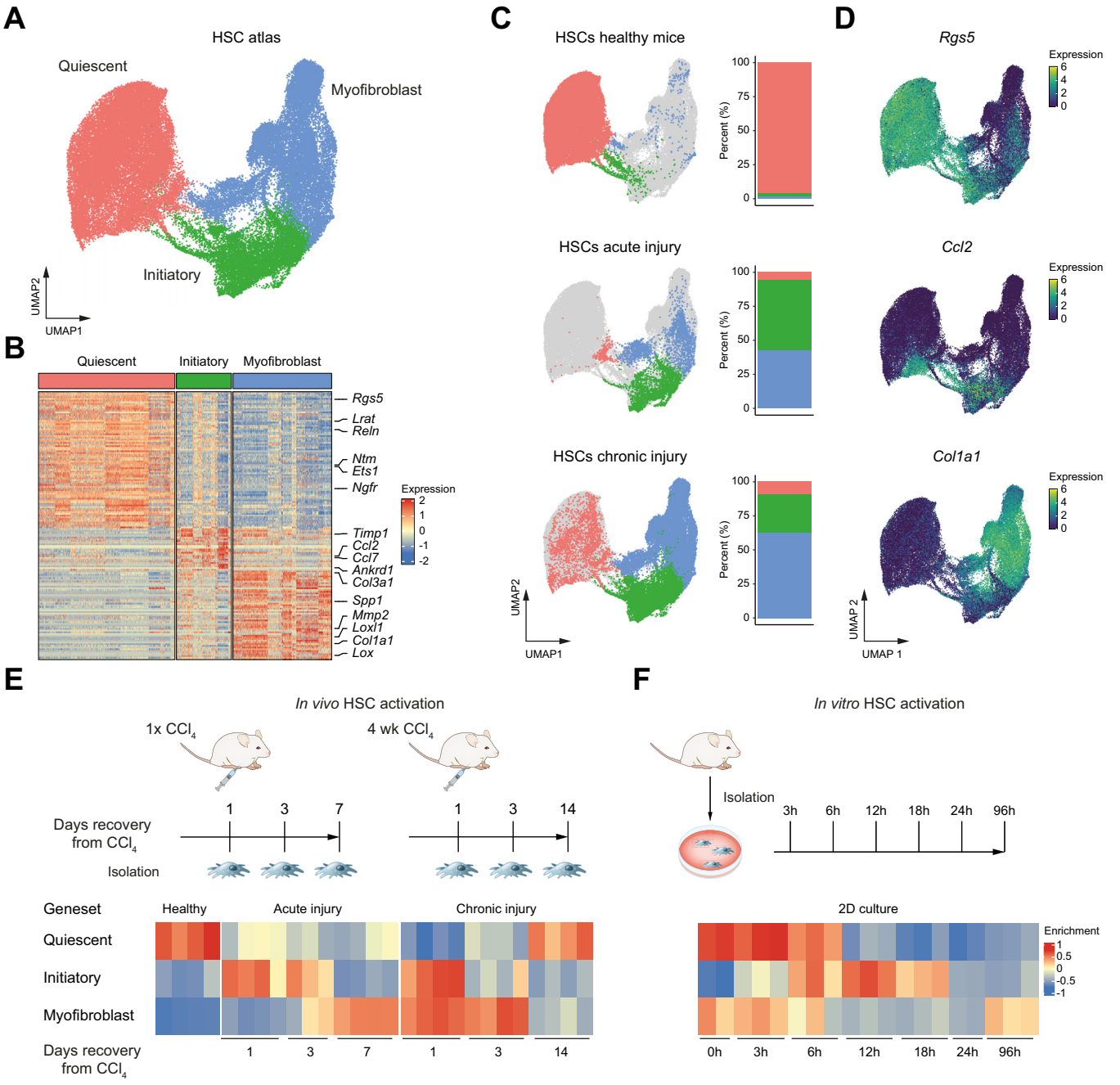

Fig. 2. Mouse HSC activation atlas and validation. (A) UMAP of mouse HSCs annotated by subtype. (B) Heatmap of 2-fold upregulated genes per subtype. (C) Location of HSCs isolated from healthy mice (n = 18) or from acutely (n = 11) or chronically injured (n = 26) mice on the UMAP and their subtype composition. (D) Normalized expression of Rgs5, Thbs1 and Col1a1. (E) GSVA of gene sets determined in B on time-resolved bulk-RNA-Seq of HSCs after an acute and chronic CCl_4 injury. (F) GSVA of gene sets determined in B on time-resolved bulk-RNA-Seq of primary mouse HSCs cultured *in vitro* (hours after plating). GSVA, gene set-variation analysis; HSCs, hepatic stellate cells; scRNA-Seq, single-cell RNA sequencing; UMAP, uniform manifold approximation and projection.

and is lost in initiatory and myofibroblast populations. This is due to the loss of most of the quiescent genes that can distinguish portal from central HSCs (Fig. S6).

The qHSC cluster was defined by high expression of conventional quiescent genes *Lrat*, *Reln* and *Rgs5* (Fig. 2B,D).[2,11,18] qHSCs highly express *Ecm1*, which stabilises TGF-β in its inactive form thereby preventing activation of HSCs, while a knockout of ECM1 leads to spontaneous liver fibrosis and death after 2 months (Fig. S7A–B).[19] Other quiescent cluster genes include the G-protein coupled receptors *Pth1r*, *Vipr1*, *Calcrl*, *Agtr1a*, *Adra2b* and *Ednrb*. Finally, the transcription factor *Ets1*, that can regulate the quiescent phenotype of HSCs,[20] was also highly expressed in this cluster. All these qHSC genes show a decreased expression upon HSC activation in each of the investigated injuries (Fig. S4B).

The initiatory HSC cluster was defined by high expression of *Ankrd1* and *Thbs1*, direct downstream targets of YAP, which is crucial for initiation of HSC activation.[21,22] Initiatory HSCs also

highly express *Ccl2*, *Ccl7* and *Cxcl10*, chemoattractant cytokines that recruit leukocytes. Myofibroblasts were defined by high expression of genes related to extracellular structure organization; upregulation of collagens 1a1, 1a2, 3a1, 5a2, 15a1 and 6a2, as well as hallmarks of activation *Lox*, *Loxl1*, *Mmp2* and *S100a6*. These markers indicate the shift from qHSCs to myofibroblasts in each of the investigated liver injuries (Fig. S4B). The commonly used HSC activation marker *Acta2* is increased in both initiatory HSCs and myofibroblasts and thus is not part of any gene set (Fig. S8). Even though independent

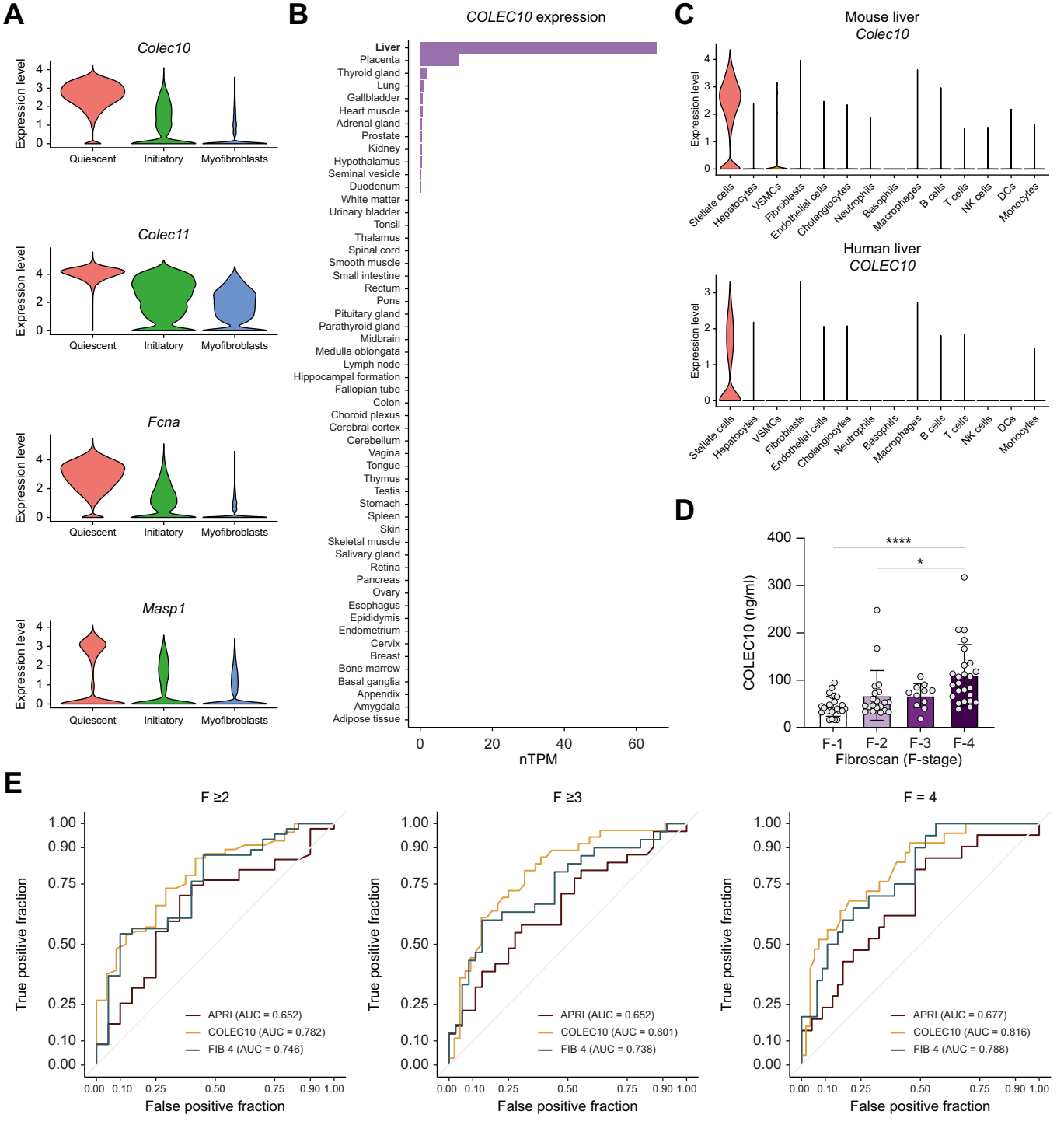

Fig. 3. COLEC10 plasma levels correlate with the extent of liver fibrosis. (A) Normalized expression of genes from the lectin complement pathway. (B) Normalized expression of *COLEC10* in human tissues based on E-MTAB-2836.[27] (C) Normalized expression of *COLEC10* in liver cell types based on GSE192742.[26] (D) Protein levels of COLEC10 determined by ELISA on plasma collected from patients suffering from chronic liver disease with different stages of liver fibrosis (n = 80). Analysis of variance test followed by Tukey's multiple comparisons test. **p* <0.05, *****p* <0.0001. (E) Receiver-operating characteristic curves of plasma COLEC10 levels and the APRI and FIB-4 score in a heterogeneous patient population at different F-stages; significant fibrosis (F ≥2), advanced fibrosis (F ≥3), and cirrhosis (F = 4).

scRNA-Seq studies have identified similar quiescent HSC and myofibroblast populations in different injury settings, the initiatory cluster only shows a partial overlap with the stage 1 activating HSCs in the study of Yang *et al.* (Fig. S9). The dynamic regulation of the three HSC subtypes could also be demonstrated using a recent single-nuclei RNA-Seq HSC dataset of mice challenged with a single APAP injection (Fig. S10 representing 13 timepoints).[23]

Next, we validated these gene sets by gene set variation analysis during time-resolved HSC activation *in vivo*. Fig. 2E shows that the quiescent gene set is enriched in healthy HSCs and in HSCs after a 14-day recovery from a chronic CCl_4 injury.[24] The initiatory gene set is enriched 1 day after a single CCl_4 injection and 1 day after chronic CCl_4 injections, confirming that initiation of HSC activation still occurs in chronically injured livers.[24] The myofibroblast gene set is enriched 7 days after a single CCl_4 injection or during chronic CCl_4 injury. During *in vitro* HSC activation we could only show a sequential enrichment of the quiescent and initiatory gene sets (Fig. 2F). The myofibroblast gene set was not enriched over time compared to freshly isolated HSCs, confirming earlier studies that culture-induced HSC activation is not equal to *in vivo* HSC activation[15,21,25] (Fig. S11A and B). Culture-induced activation of primary human HSCs confirms the discrepancy between these different models and species at the single gene level (Fig. S11C). This was confirmed by further analysis of the expression of individual genes in the myofibroblast gene set which show upregulation *in vivo* but downregulation during *in vitro* HSC activation (Fig. S12).

COLEC10 is a potential biomarker for liver fibrosis

We found several components of the lectin complement pathway (*Colec10*, *Colec11*, *Fcna* and *Masp1*) to only be expressed in qHSCs (Fig. 3A). Further investigation revealed that *COLEC10* is predominantly expressed in the liver compared to other organs (Fig. 3B). In the liver, *COLEC10* is primarily expressed by HSCs (Fig. 3C),[26] indicating that *COLEC10* is nearly exclusively expressed by qHSCs.

Since COLEC10 is a secreted protein, we investigated the levels of *COLEC10* in the plasma of patients suffering from different stages of liver fibrosis (Table S4). Surprisingly, and in contrast to the decreased expression of *COLEC10* mRNA in myofibroblasts, the plasma concentration of COLEC10 increases in patients with more severe liver fibrosis (Fig. 3D and Fig. S13A). To investigate this discrepancy we evaluated whether other cell types in an injured liver express COLEC10, but this was not the case (Fig. S13B). The decrease of *COLEC10* RNA during HSC activation occurs in all investigated liver injuries, both in mice and humans, and during *in vitro* activation (Fig. S13C–E). In livers of mice subjected to chronic CCl_4 injury there was also an increase of COLEC10 protein levels while a decrease in *COLEC10* mRNA levels was observed (Fig. S13F–H). The discrepancy in COLEC10 protein and mRNA levels might be caused by a drastic increase in translation during HSC activation as genes coding for ribosomal proteins are highly upregulated (Fig. S13I–J). This increased translation may produce more Colec10 protein even though the mRNA levels are lower. Additionally, comparison of the area under the receiver-operating characteristic curves shows that plasma levels of *COLEC*10 exhibited superior discriminative ability compared to the FIB-4 and APRI scores in predicting fibrosis stage of these patients with CLD (Fig. 3E, Table S5). These results highlight the potential of *COLEC10* plasma levels as a very effective biomarker for liver fibrosis.

Human HSC activation atlas

Next, we evaluate if the HSC subtypes and their gene sets are relevant for human disease by constructing a human HSC activation atlas using a similar approach as for the murine HSC atlas. We integrated the mesenchymal cells of three publicly available scRNA-Seq datasets based on healthy livers as well as livers from patients suffering from Crigler-Najjar, obesity and cirrhosis (Table S2).[10–12] This time we extracted the HSCs from the mesenchymal cells based on DCN expression (Fig. S14). The human HSC atlas contains 774 cells and can be clustered into quiescent HSCs, initiatory HSCs and myofibroblasts as well (Fig. 4A, B). These human HSC subtypes express similar genes as the mouse HSC subtypes (Fig. S15A and B); qHSCs express canonical markers (*RELN, ECM1* and *RGS5*), G-protein coupled receptors (*VIPR1*, *CALCRL*, *EDNRB*, *AGTR1* and *PTH1R*) as well as *FCN1*, *COLEC10* and *COLEC11*. The human initiatory HSCs show high expression of the chemoattractant cytokine CCL2, the direct YAP target THBS1 as well as TIMP1. The human myofibroblasts are characterized by S100A6, WT1 and C3. Enrichment analysis of the mouse HSC gene sets in the human atlas shows that the quiescent and myofibroblast gene sets are both clearly enriched in their human HSC subtype counterpart, suggesting that these HSC stages are conserved between organisms. However, this effect was less clear for the initiatory subtype (Fig. 4C). Expression of the single genes *RGS5*, *CCL2* and *COL1A1*, representative for the three mouse clusters, was also enriched in the three human HSC clusters, albeit less pronounced (Fig. 4D). The three subtypes could also be distinguished by label transfer in a recent single-nuclei RNA-Seq dataset of healthy human livers and livers with acute liver failure, displaying similar gene expression patterns (Fig. S16).[23]

Transcription factors driving HSC activation are conserved between liver injuries and species

Next, we identified the TFs driving the differentiation from qHSCs to myofibroblasts. We determined the most active TFs for each HSC subtype using pySCENIC which predicts TF activity (indicated with (+) sign) based on co-expression of TFs and their potential target genes, further filtered for cis-regulatory TF motifs present in the target genes.[28] qHSCs show high activity of nuclear receptors *Rxra*, *Nr1h4* and *Nr3c1*, all associated with HSC quiescence[29] (Fig. 5A). The predicted top 15 quiescent TFs also includes *Ets1* and *Ets2*, TFs previously implicated in HSC identity and quiescence.[20] *Foxf1*, a TF active during HSC development without which stellate cells show impaired activation, was also highly active in the qHSC cluster.[30]

Members of the activator protein-1 (AP-1) family such as *Fosl1* and *Fosl2*, as well as several members of the Nfkβ-family (*Nfkb1*, *Nfkb2*, *Relb*), were highly active in initiatory HSCs confirming their role in HSC activation[31,32] (Fig. 5A). Additionally, the early growth response (Egr) TF family was predicted to be crucial for HSC initiation as *Egr3* and *Egr2* both show high

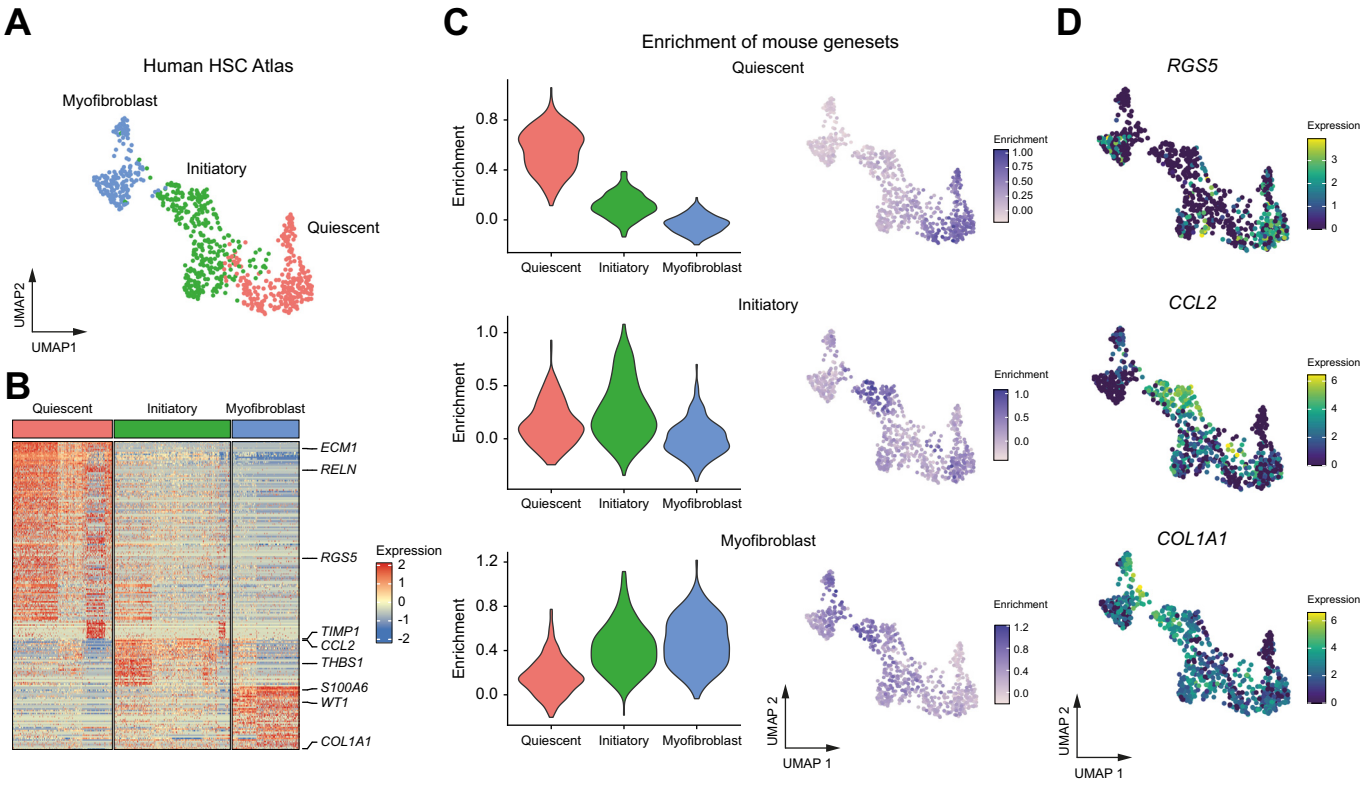

Fig. 4. Humane HSC activation atlas. (A) UMAP of human HSCs annotated by subtype. (B) Heatmap of >2-fold upregulated genes per subtype. (C) Gene set enrichment of murine HSC gene sets in the integrated human HSC dataset. (D) Normalized expression of *RGS5*, *CCL2* and *COL1A1*. HSCs, hepatic stellate cells; UMAP, uniform manifold approximation and projection.

TF activity. In the myofibroblast cluster, transcription factors *Wt1*, *Prrx1* and *Mef2c* were highly active (Fig. 5A), confirming their suggested role during HSC activation.[33–35]

To determine whether the TF activity pattern responsible for the gradual differentiation from qHSCs towards myofibroblasts is conserved between mouse and human HSCs, we used trajectory inference on the SCENIC results to order the TF activities in pseudotime in both the mouse and human HSC activation atlas (Fig. 5B). LOESS regression shows that in both mice and humans, the top three quiescent TFs (RXRA, FOXF1, NR1H4) become less active and the myofibroblast TFs (WT1, PRRX1) become more active during HSC activation, while the activities of the top three initiatory TFs (FOSL1, EGR3, NFKB2) peak somewhere in between (Fig. 5B). Only MEF2C activity could not be identified in the human datasets, possibly due to the low number of cells in the human HSC atlas. The predicted TF activities of TFs outside of the top three are visualized per human HSC subtype in Fig. S15C.

Since the TF activity patterns seem to be conserved between human and mouse HSC activation, we determined whether they are also conserved between models of liver injury. The top 15 subtype-specific TFs indeed show a conserved pattern in all investigated liver injuries (Fig. S17). We then modelled the TF activities along pseudotime for each liver injury dataset, using tradeseq.[36] Using this approach, we could not show any significant differences in TF activity patterns between different liver models for the quiescent TFs (*Rxra*, *Foxf1* and *Nr1h4*), initiatory TFs (*Fosl1*, *Egr3* and *Nfkb2*) or myofibroblast TFs (*Wt1*, *Prrx1* and *Mef2c*) (Fig. 5C). Taken together this suggests that the TFs driving HSC activation are independent of liver injury.

Ligands inducing HSC activation are conserved between liver aetiologies

Next, we asked whether the upstream signalling events that drive HSC activation are conserved between different liver injury models using NicheNet. NicheNet calculates the probability that a certain ligand regulates the transcription of genes based on prior knowledge of ligand-receptor interactions, signal transduction and TF-target gene interactions.[37] To enhance this prediction, we added the mouse HSC-specific TF-target gene interactions determined by pySCENIC to the prior knowledge in the standard NicheNet workflow (Fig. 6A). Using this approach, we identified ligands that have a high potential to induce genes upregulated in the myofibroblast cluster compared to the quiescent cluster in the HSC activation atlas (Fig. 6A). Not surprisingly, within the top 10 predicted ligands responsible for HSC activation *in vivo* we found TGF-β1, AGT, TGF-β3 and SPP1,[38–40] all known mediators of HSC activation (Fig. 6B,C). TGF-β1 is predicted to induce the expression of collagens, Lysyl oxidases and ligands that can further drive HSC activation (*Igf1* and *Spp1*) (Fig. 6B, Fig. S7C-D). In fact, TGF-β is the top ligand to induce the shift in transcriptional landscape that leads to HSC activation in every liver injury analysed, except in the acute CCl_4 injury model where it places second (Supplementary file 3, Fig. 6C). Similarly, *Spp1* and *Egf* are top-ranked in almost all liver injuries (Fig. 6C). Together, this

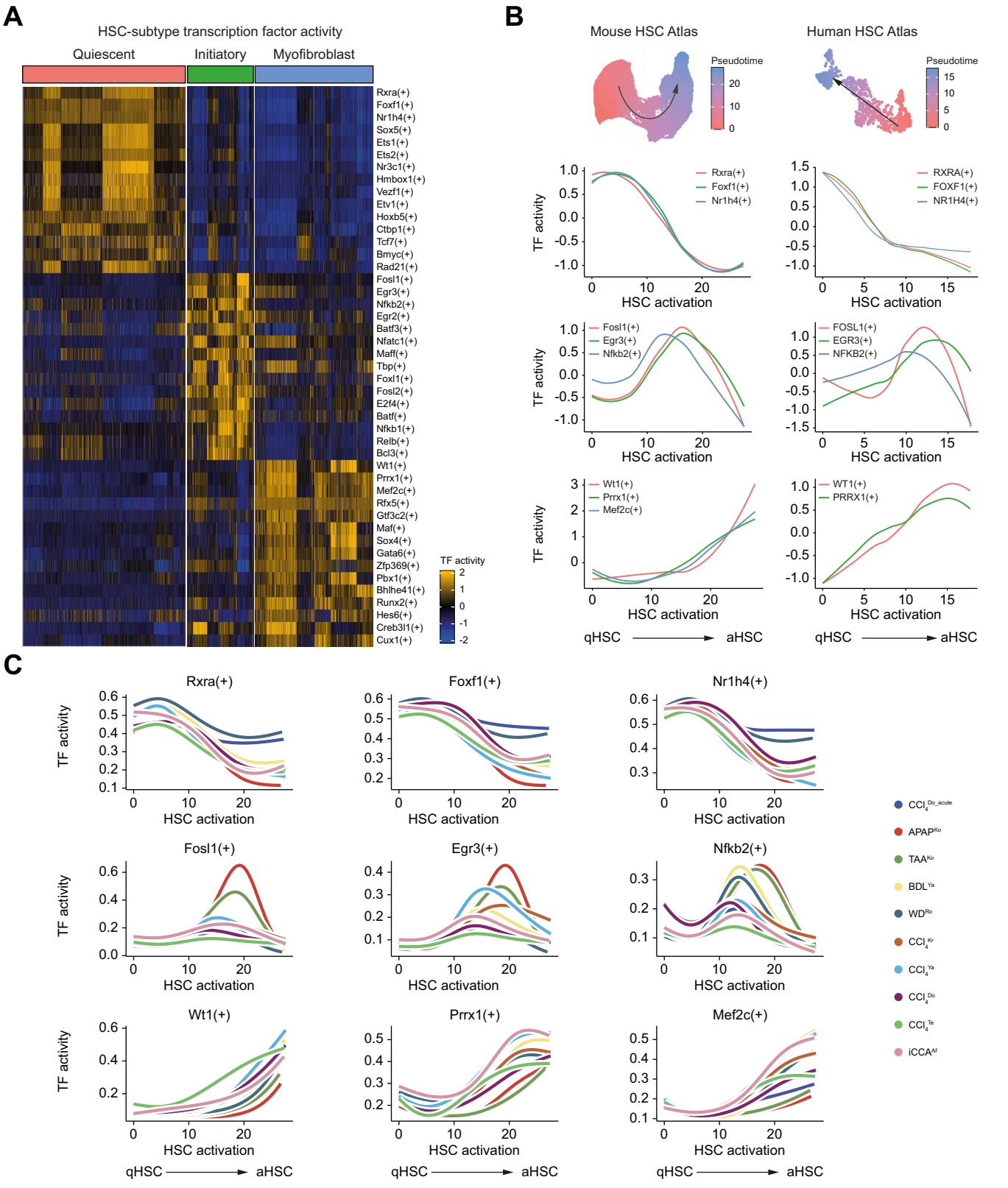

Fig. 5. Transcription factor activity during HSC activation is conserved between different disease aetiologies and between mice and human. (A) Heatmap of the TF activity of the top 15 active TFs per HSC subtype. (B) Pseudotime derived from the trajectory inference for the mouse and human integrated HSC activation atlas. Activity patterns of the top three TFs for each subtype in function of pseudotime by LOESS regression. (C) General additive models fit for selected TF activities in each mouse liver injury dataset. HSCs, hepatic stellate cells; TFs, transcription factors.

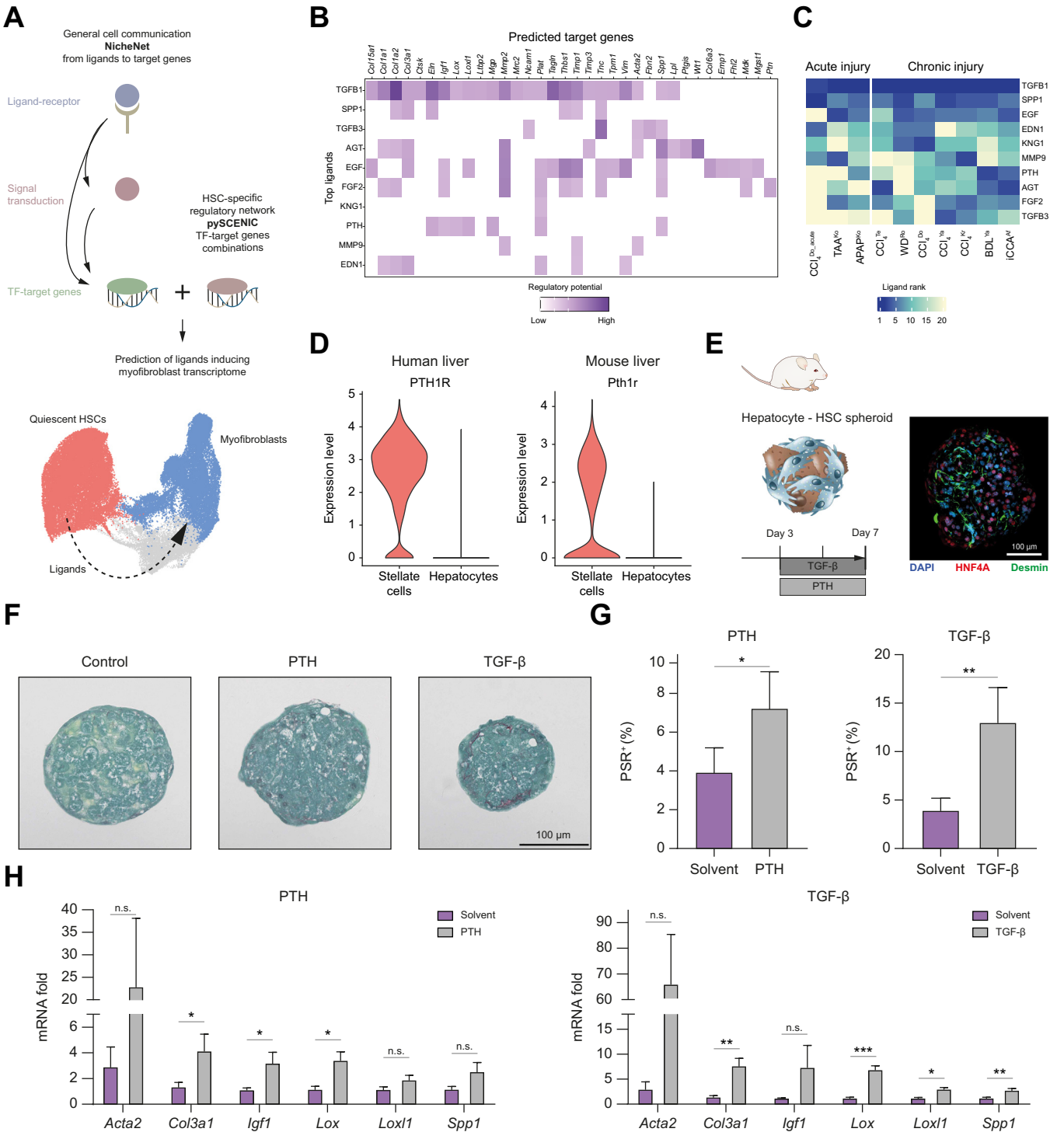

Fig. 6. Ligand prediction of HSC activation and identification of parathyroid hormone as a novel ligand. (A) Schematic overview: The NicheNet ligand prediction is based on prior knowledge of ligand-receptor interactions, intermediate signalling steps and TF target gene interactions from all possible cell types. This prior knowledge was complemented with HSC-specific TF target gene interactions as found by the pySCENIC algorithm to predict the ligands inducing the differentially expressed genes of myofibroblasts compared to qHSCs. (B) Downstream target genes for the top 10 ligands inducing the differentiation from qHSCs to myofibroblasts. (C) Top 10 predicted ligands based on merged HSC activation atlas (y-axis) and the rank of these ligands when top ligands are predicted in each liver injury dataset separately (x-axis). (D) Normalized expression of the parathyroid hormone receptor Pth1r in HSCs and hepatocytes based on GSE192742.[26] (E) Schematic overview of experimental setup testing the effect of parathyroid hormone and TGF-β on primary mouse liver spheroids. HNF4A and Desmin expression at day 7 in mouse HSC-hepatocyte spheroids. (F) Sirius-red staining of spheroids treated with 80 nM parathyroid hormone, 5 ng/ml TGF-β or solvent. (G) Quantification of Sirius red-positive area in the spheroids. The difference between the treatments was tested with a one-tailed paired t test. *p <0.05, **p <0.01, n = 5. (H) Relative expression of HSC activation genes in spheroids treated with 80 nM parathyroid hormone or 5 ng/ml TGF-β. The difference between the treatments was tested with a one-tailed paired t test. *p <0.05, **p <0.01, ***p <0.001, n = 5. (q)HSCs, (quiescent) hepatic stellate cells; TFs, transcription factors; PTH, parathyroid hormone.

indicates that the signalling events leading to HSC activation in mouse models of liver injury are conserved and are independent of the underlying aetiology. Most of the top 10 ligands predicted to induce HSC activation in mice were also in the top 40 predicted ligands inducing HSC activation in the human HSCs and vice versa (Fig. S15C). Interestingly, the analysis also predicted novel HSC activating ligands such as parathyroid hormone (*Pth*) to be driving HSC activation in most liver injuries.

Since a high-level of parathyroid hormone is significantly associated with MASLD and the receptor for parathyroid hormone is predominantly expressed in HSCs in the liver (Fig. 6D),[26,41] we decided to validate if parathyroid hormone can induce HSC activation. We exposed spheroids consisting of primary mouse HSCs and hepatocytes to 80 nM parathyroid hormone or 5 ng/ml TGF-β (Fig. 6E,F). Spheroids treated with parathyroid hormone had increased expression of HSC activation genes and increased cross-linked collagen formation compared to control spheroids (Fig. 6H, I). Although less potent than TGF-β, these results suggest that parathyroid hormone can contribute to formation of fibrosis by inducing HSC activation.

Tools to annotate and interrogate HSC subtypes

Since we can successfully predict HSC subtypes using the mouse HSC atlas on single-nuclei RNA-Seq data of mouse and human livers (Figs. S12 and S16), we also validated that label transfer on an scRNA-seq dataset of HSCs obtained from mice subjected to chronic CCl_4 injections[22] was able to correctly distinguish the HSC subtypes (Fig. S18). To facilitate the annotation of mesenchymal- and HSC-subtypes we developed a tool that projects any single-cell or single-nuclei RNA-Seq dataset onto the mesenchymal cell atlas and the HSC activation atlas (10.5281/zenodo.10512657). As an example, we used the data from Filliol *et al.* 2022[22] and Matchett *et al.* 2024[23] (Figs. S12 and S18) which were correctly annotated using this tool (Fig. S19). Finally, we provide an interactive browser to interrogate the mouse and human HSC single-cell atlas for gene expression and TF activity (https://livr.research.vub.be/singlecellatlas).

Discussion

Activated HSCs are responsible for the vast majority of matrix deposited during any given chronic liver injury and are the main source of cancer-associated fibroblasts in liver cancers.[9,42] However, it was unclear whether the mechanisms that drive the activation of HSCs are similar in different disease settings. In this study we merged 10 datasets, covering seven different liver injury settings in mice, and generated the very first mouse single-cell HSC atlas. We identified three HSC subtypes that are present in all liver injury models in mice and are conserved in human livers; qHSCs, initiatory HSCs and myofibroblasts. Our analysis shows for the first time that the ligands and TFs that drive HSC activation are highly conserved between different liver injury models. Finally, we interrogated the single-cell HSC atlas and could identify COLEC10 as a highly specific HSC marker that can be used as a biomarker of fibrosis and demonstrated that parathyroid hormone has HSC-activating properties.

At the onset of this study, we hypothesized that variations in hepatic injury might lead to distinct HSC activation mechanisms, enabling the identification of, for instance, "biliary injury" or "cancer-mediated" TFs that would regulate HSC activation. Surprisingly, our findings refute this hypothesis, as the key TFs governing the different HSC stages appear to be highly similar across all injury settings. The top TFs driving HSC activation are highly similar in HSCs isolated from livers where fibrosis is evident, *i.e.* mice exposed for multiple weeks to CCl_4,[2,4,6,8] when compared to HSCs isolated from acutely injured or western diet-fed mice, which exhibit only minor fibrosis.[2,3,7]

The unbiased pySCENIC analysis identified *Rxra*, *Foxf1* and *Nr1h4* as TFs crucial for the maintenance of the qHSC state in mouse and human livers (Fig. 5). Previous studies provided solid evidence that these TFs indeed have the potential to regulate HSC activation. Agonists for *Rxr*-isoforms inhibit proliferation and reduce the expression of collagens in HSCs.[43] *Foxf1* is expressed in foetal and adult HSCs and prevents excessive collagen production in HSCs and myofibroblasts.[30] Agonists of *Nr1h4* reduce fibrosis after *in vivo* liver injury as well as reduce HSC activation *in vitro*.[44] The effect of *Nr1h4* agonists, such as obeticholic acid, on CLD progression has been investigated in clinical trials.[45]

Our study further suggests that *Fosl1*, *Egr3* and *Nfkb2* are TFs that drive the initiation phase of HSC activation. *Fosl1* is part of the AP-1 family and is known to be associated with HSC activation.[31] Members of the Egr TF family play an important role in the TGF-β-dependent fibrotic response in multiple organs. While *Egr1* has been the focus of anti-fibrotic studies, we show that the activity of *Egr2* and *Egr3* is increased during the initiation of HSC activation and not *Egr1*, thereby confirming their non-redundant functions in fibrosis (Fig. S20).[46] The third most active TF in the initiatory cluster was NF-κβ2. Activation of the NF-κB complex has been linked to the activation of HSCs.[32] Furthermore, the interaction between AP-1, NF-kB and other inflammatory mediators has been suggested as a potential target to combat CLD.[47] Thus, our analysis reinforces the significance of inhibiting AP-1 and NF-κB as a valid approach to combat fibrosis because it could block the earliest events of HSC activation in all liver injury settings, acute and chronic.

The myofibroblast TF cluster showed high activities of *Wt1*, *Prrx1* and *Mef2c* across all liver injury models. These three TFs are known regulators of *Col1a1* in activated HSCs.[33–35] Although we could only detect WT1 and PRRX1 in the analysed human dataset, both their activities were enhanced at the myofibroblast stage (Fig. 5). Strikingly, even cancer-associated fibroblasts seem to depend on the same TFs to reach their activated state as HSCs activated in CCl_4 injury settings. Indeed, recent studies have shown that qHSCs, which express protective factors, shift towards activated HSCs/cancer-associated fibroblasts expressing tumour-promoting mediators, thereby setting the stage for hepatocellular carcinoma development in CLD.[22] This suggests that inhibitors of any TF or ligand that mediates the transition from a qHSC to an activated HSC state could also impact the tumour-promoting role of cancer-associated fibroblasts, thereby enlarging the utility of such drugs for clinical use.

In addition to the top TFs being conserved during HSC activation, the ligands inducing these TFs also seem to be conserved: TGF-β, EGF, SPP1 and pre-angiotensinogen (AGT) are among the top ligands predicted to induce the activation

process in most injury datasets. Not surprisingly, as all ligands are known to induce HSC activation and both pre-angiotensinogen and TGF-β have been the subject of clinical trials for liver fibrosis.[48] Herein, we identified parathyroid hormone as a novel ligand that can induce HSC activation and confirmed its activity in primary mouse HSC-hepatocyte spheroid cultures. The pro-fibrotic potential of parathyroid hormone was recently demonstrated in the CCl_4 mouse model, and our analysis suggests that it most likely also plays a role in other injury settings.[49]

This study also provides fundamental insight into HSC biology. Analysis of the HSC subtypes led to the identification of genes with distinct expression patterns in HSC activation that are relatively understudied. Specific genes from the lectin complement pathway turn out to be excellent qHSC markers. Most striking is the expression of *Colec10*, which is almost exclusively expressed in the liver (Fig. S21A) and solely in HSCs (Fig. S21B). We could demonstrate that COLEC10 is a potential biomarker of liver fibrosis, outperforming FIB4 and APRI in this cohort of patients suffering from liver disease with different aetiologies, confirming recent findings.[50] At this moment, we cannot exclude that COLEC10 is expressed in non-hepatic tissues in patients with CLD. Future testing in independent larger cohorts will show whether COLEC10 can be used as a biomarker in a clinical setting. At the fundamental level, *COLEC10* has tremendous potential as a cell type-specific promoter in lineage tracing and conditional knockout studies when compared to currently used CRE-lines like *Lrat*, *Gfap* or *Tcf21* (Fig. S21). The role of the lectin complement pathway in HSC biology is still unclear. We find that while *Colec10*, *Colec11*, *Masp1* and *Fcna* are highly enriched in qHSCs, the main effector of all complement pathways *C3* is barely expressed in quiescent cells and induced upon HSC activation, suggesting that *Colec10*, *Colec11*, *Masp1* and *Fcna* could have other functions beyond complement activation in HSCs, warranting further investigation (Figs S11A,C and S12A).

In conclusion, through comparison of the transcriptome of HSCs from multiple disease models in mice and humans we delineate a common HSC activation trajectory that holds true across species and liver injuries. The HSC activation atlas presented here has the potential to provide novel insights into liver fibrosis and steer novel treatment or surveillance options for patients suffering from CLD. Lastly, since the regulatory network of HSC activation is conserved, any liver injury model in mice can be used to discover or evaluate anti-fibrotic drugs targeting HSCs.

Affiliations

[1]*Vrije Universiteit Brussel, Liver Cell Biology research group, Laarbeeklaan 103, 1090 Brussel, Belgium;* [2]*Department of Gastro-Enterology and Hepatology, Universitair Ziekenhuis Brussel, Brussels, Belgium*

Abbreviations

APAP, acetaminophen; BDL, bile duct ligation; CCl_4, carbon tetrachloride; CLD, chronic liver disease; (q)HSCs, (quiescent) hepatic stellate cells; MASLD, metabolic dysfunction-associated steatotic liver disease; scRNA-Seq, single-cell RNA sequencing; TF, transcription factors.

Financial support

Stefaan Verhulst: FWO Post-doc mandate 1243121N. Leo A. van Grunsven: G042719N, G071922N and FWO-SBO-QPG-359638. Vincent De Smet: 1192920N.

Conflict of interest

There are no conflicts of interest to declare that are relevant to this work.

Please refer to the accompanying ICMJE disclosure forms for further details.

Authors' contributions

Vincent Merens: Conceptualization, Methodology, Data curation, Formal analysis, Investigation, Visualization, Writing – original draft and review & editing. Elisabeth Knetemann: Methodology, Writing – review & editing. Elif Gürbüz: Methodology. Vincent De Smet, Hendrik Reynaert: Resources, reviewing. Nouredin Messaoudi: Resources. Stefaan Verhulst: Formal analysis, Data curation, Supervision, Writing – review & editing. Leo A. van Grunsven: Conceptualization, Writing – review & editing, Funding acquisition, Project administration, Supervision, Resources.

Data availability statement

All RNAseq data is available through indicated public repositories or available upon request from the authors involved. Newly generated RNAseq data is available at the GEO database as GSE276915. Newly generated data is available through 10.5281/zenodo.10514236. Shiny App for HSC annotation through 10.5281/zenodo.10512657. Shiny App for browsing the HSC atlas for genes and transcription factors is available through https://livr.research.vub.be/rnaseq-projects.

Code availability: All R, python and QuPath scripts necessary to reproduce the analysis are available at https://github.com/LIVRlab/HSC-Activation-atlas.

Acknowledgements

We would like to thank Nathalie Eysackers for support with the isolation of the mouse HSCs and hepatocytes.

Supplementary data

Supplementary data to this article can be found online at https://doi.org/10.1016/j.jhepr.2024.101223.

References

Author names in bold designate shared co-first authorships.

[1] Asrani SK, Devarbhavi H, Eaton J, et al. Burden of liver diseases in the world. J Hepatol 2019;70(1):151–171.

[2] **Dobie R**, **Wilson-Kanamori JR**, Henderson BEP, et al. Single-cell transcriptomics uncovers zonation of function in the mesenchyme during liver fibrosis. Cell Rep 2019;29(7):1832–1847 e8.

[3] Rosenthal SB, Liu X, Ganguly S, et al. Heterogeneity of HSCs in a mouse model of NASH. Hepatology 2021;74(2):667–685.

[4] **Yang W**, **He H**, Wang T, et al. Single-cell transcriptomic analysis reveals a hepatic stellate cell-activation roadmap and myofibroblast origin during liver fibrosis in mice. Hepatology 2021;74(5):2774–2790.

[5] Iwaisako K, Jiang C, Zhang M, et al. Origin of myofibroblasts in the fibrotic liver in mice. Proc Natl Acad Sci U S A 2014;111(32):E3297–E3305.

[6] Krenkel O, Hundertmark J, Ritz TP, et al. Single cell RNA sequencing identifies subsets of hepatic stellate cells and myofibroblasts in liver fibrosis. Cells 2019;8(5).

[7] Kolodziejczyk AA, Federici S, Zmora N, et al. Acute liver failure is regulated by MYC- and microbiome-dependent programs. Nat Med 2020;26(12):1899–1911.

[8] Terkelsen MK, Bendixen SM, Hansen D, et al. Transcriptional dynamics of hepatic sinusoid-associated cells after liver injury. Hepatology 2020;72(6):2119–2133.

[9] Affo S, Nair A, Brundu F, et al. Promotion of cholangiocarcinoma growth by diverse cancer-associated fibroblast subpopulations. Cancer Cell 2021;39(6):866–882 e11.

[10] Payen VL, Lavergne A, Alevra Sarika N, et al. Single-cell RNA sequencing of human liver reveals hepatic stellate cell heterogeneity. JHEP Rep 2021;3(3):100278.

[11] Ramachandran P, Dobie R, Wilson-Kanamori JR, et al. Resolving the fibrotic niche of human liver cirrhosis at single-cell level. Nature 2019;575(7783):512–518.

[12] **Fred RG**, **Steen Pedersen J**, Thompson JJ, et al. Single-cell transcriptome and cell type-specific molecular pathways of human non-alcoholic steatohepatitis. Sci Rep 2022;12(1):13484.

[13] Sachs MC. plotROC: a tool for plotting ROC curves. J Stat Softw 2017;79.

[14] **van Os EA**, **Cools L**, Eysackers N, et al. Modelling fatty liver disease with mouse liver-derived multicellular spheroids. Biomaterials 2022;290:121817.
[15] Mannaerts I, Eysackers N, Anne van Os E, et al. The fibrotic response of primary liver spheroids recapitulates in vivo hepatic stellate cell activation. Biomaterials 2020;261:120335.
[16] Bankhead P, Loughrey MB, Fernandez JA, et al. QuPath: open source software for digital pathology image analysis. Sci Rep 2017;7(1):16878.
[17] Leite SB, Roosens T, El Taghdouini A, et al. Novel human hepatic organoid model enables testing of drug-induced liver fibrosis in vitro. Biomaterials 2016;78:1–10.
[18] Mederacke I, Hsu CC, Troeger JS, et al. Fate tracing reveals hepatic stellate cells as dominant contributors to liver fibrosis independent of its aetiology. Nat Commun 2013;4:2823.
[19] Fan W, Liu T, Chen W, et al. ECM1 prevents activation of transforming growth factor beta, hepatic stellate cells, and fibrogenesis in mice. Gastroenterology 2019;157(5):1352–1367 e13.
[20] Liu X, Xu J, Rosenthal S, et al. Identification of lineage-specific transcription factors that prevent activation of hepatic stellate cells and promote fibrosis resolution. Gastroenterology 2020;158(6):1728–1744 e14.
[21] **Mannaerts I**, **Leite SB**, Verhulst S, et al. The Hippo pathway effector YAP controls mouse hepatic stellate cell activation. J Hepatol 2015;63(3):679–688.
[22] Filliol A, Saito Y, Nair A, et al. Opposing roles of hepatic stellate cell subpopulations in hepatocarcinogenesis. Nature 2022;610(7931):356–365.
[23] Matchett KP, Wilson-Kanamori JR, Portman JR, et al. Multimodal decoding of human liver regeneration. Nature 2024;630(8015):158–165.
[24] De Smet V, Eysackers N, Merens V, et al. Initiation of hepatic stellate cell activation extends into chronic liver disease. Cell Death Dis 2021;12(12):1110.
[25] De Minicis S, Seki E, Uchinami H, et al. Gene expression profiles during hepatic stellate cell activation in culture and in vivo. Gastroenterology 2007;132(5):1937–1946.
[26] **Guilliams M**, **Bonnardel J**, **Haest B**, et al. Spatial proteogenomics reveals distinct and evolutionarily conserved hepatic macrophage niches. Cell 2022;185(2):379–396 e38.
[27] Uhlen M, Fagerberg L, Hallstrom BM, et al. Proteomics. Tissue-based map of the human proteome. Science 2015;347(6220):1260419.
[28] **Van de Sande B**, **Flerin C**, Davie K, et al. A scalable SCENIC workflow for single-cell gene regulatory network analysis. Nat Protoc 2020;15(7):2247–2276.
[29] Pu S, Zhou H, Liu Y, et al. Roles of nuclear receptors in hepatic stellate cells. Expert Rev Gastroenterol Hepatol 2021;15(8):879–890.
[30] Flood HM, Bolte C, Dasgupta N, et al. The Forkhead box F1 transcription factor inhibits collagen deposition and accumulation of myofibroblasts during liver fibrosis. Biol Open 2019;8(2).
[31] Bahr MJ, Vincent KJ, Arthur MJ, et al. Control of the tissue inhibitor of metalloproteinases-1 promoter in culture-activated rat hepatic stellate cells: regulation by activator protein-1 DNA binding proteins. Hepatology 1999;29(3):839–848.
[32] Liu C, Chen X, Yang L, et al. Transcriptional repression of the transforming growth factor beta (TGF-beta) Pseudoreceptor BMP and activin membrane-bound inhibitor (BAMBI) by Nuclear Factor kappaB (NF-kappaB) p50 enhances TGF-beta signaling in hepatic stellate cells. J Biol Chem 2014;289(10):7082–7091.
[33] Yang YM, Noureddin M, Liu C, et al. Hyaluronan synthase 2-mediated hyaluronan production mediates Notch1 activation and liver fibrosis. Sci Transl Med 2019;11(496).
[34] Jiang F, Stefanovic B. Homeobox gene Prx1 is expressed in activated hepatic stellate cells and transactivates collagen alpha1(I) promoter. Exp Biol Med (Maywood) 2008;233(3):286–296.
[35] Wang X, Tang X, Gong X, et al. Regulation of hepatic stellate cell activation and growth by transcription factor myocyte enhancer factor 2. Gastroenterology 2004;127(4):1174–1188.
[36] Van den Berge K, Roux de Bezieux H, Street K, et al. Trajectory-based differential expression analysis for single-cell sequencing data. Nat Commun 2020;11(1):1201.
[37] Browaeys R, Saelens W, Saeys Y. NicheNet: modeling intercellular communication by linking ligands to target genes. Nat Methods 2020;17(2):159–162.
[38] Hellerbrand C, Stefanovic B, Giordano F, et al. The role of TGFbeta1 in initiating hepatic stellate cell activation in vivo. J Hepatol 1999;30(1):77–87.
[39] **Moreno M**, **Gonzalo T**, Kok RJ, et al. Reduction of advanced liver fibrosis by short-term targeted delivery of an angiotensin receptor blocker to hepatic stellate cells in rats. Hepatology 2010;51(3):942–952.
[40] **Urtasun R**, **Lopategi A**, George J, et al. Osteopontin, an oxidant stress sensitive cytokine, up-regulates collagen-I via integrin alpha(V)beta(3) engagement and PI3K/pAkt/NFkappaB signaling. Hepatology 2012;55(2):594–608.
[41] Jaroenlapnopparat A, Rittiphairoj T, Chaisidhivej N, et al. High parathyroid hormone level as a marker of non-alcoholic fatty liver disease and non-alcoholic steatohepatitis: a systematic review and meta-analysis. Diabetes Metab Syndr 2023;17(8):102827.
[42] Bhattacharjee S, Hamberger F, Ravichandra A, et al. Tumor restriction by type I collagen opposes tumor-promoting effects of cancer-associated fibroblasts. J Clin Invest 2021;131(11).
[43] Wang Z, Xu J, Zheng Y, et al. Effect of the regulation of retinoid X receptor-alpha gene expression on rat hepatic fibrosis. Hepatol Res 2011;41(5):475–483.
[44] Fiorucci S, Antonelli E, Rizzo G, et al. The nuclear receptor SHP mediates inhibition of hepatic stellate cells by FXR and protects against liver fibrosis. Gastroenterology 2004;127(5):1497–1512.
[45] Ratziu V, Sanyal AJ, Loomba R, et al. REGENERATE: design of a pivotal, randomised, phase 3 study evaluating the safety and efficacy of obeticholic acid in patients with fibrosis due to nonalcoholic steatohepatitis. Contemp Clin Trials 2019;84:105803.
[46] Fang F, Shangguan AJ, Kelly K, et al. Early growth response 3 (Egr-3) is induced by transforming growth factor-beta and regulates fibrogenic responses. Am J Pathol 2013;183(4):1197–1208.
[47] Liu T, Zhou Y, Ko KS, et al. Interactions between myc and mediators of inflammation in chronic liver diseases. Mediators Inflamm 2015;2015:276850.
[48] Guo YC, Lu LG. Antihepatic fibrosis drugs in clinical trials. J Clin Transl Hepatol 2020;8(3):304–312.
[49] Hong T, Xiong X, Chen Y, et al. Parathyroid hormone receptor-1 signaling aggravates hepatic fibrosis through upregulating cAMP response element-binding protein-like 2. Hepatology 2023;78(6):1763–1776.
[50] **Zhang M**, **Jing Y**, Xu W, et al. The C-type lectin COLEC10 is predominantly produced by hepatic stellate cells and involved in the pathogenesis of liver fibrosis. Cel Death Dis 2023;14(11):785.

Keywords: Chronic liver disease; single-cell RNA-Sequencing; parathyroid hormone; COLEC10.
Received 4 March 2024; received in revised form 13 September 2024; accepted 17 September 2024; Available online 20 September 2024